Proc. Estonian Acad. Sci. Engng., 1997, **3**, 3, 185–195
https://doi.org/10.3176/eng.1997.3.04

# DESIGN OF THE ELASTIC DOUBLE-SPIRAL STRIP UNDER LOCAL LOADING

Mati HEINLOO and Margus KÜLASALU

Department of Mechanics and Machine Design, Estonian Agricultural University, Kreutzwaldi 58a, EE-2400 Tartu, Estonia

Received 23 December 1996, revised 11 April 1997, accepted 15 May 1997

**Abstract.** This paper considers an elastic double-spiral strip of constant or piecewise constant thickness. One end of this strip is rigidly clamped and the other is loaded by force. Using the Finite Element Method Program ANSYS 5.0A, the paper studies the dependence of displacements, the maximum of the von Mises stress and the angle (cutting angle) between tangent on the strip's loaded end and the opposite direction of the force on the geometrical parameters of the strip. By the optimal design technique of ANSYS 5.0A, the piecewise constant distribution of strip thickness, which minimizes its volume, has been found. The von Mises stress, displacements and the cutting angle for the strip of constant thickness and for that of piecewise constant thickness of the minimum volume were compared. The results of the present paper can be used for seedbed cultivator *s*-tines.

**Key words:** elastic strip, finite element method, optimal design, seedbed cultivator *s*-tines.

## 1. INTRODUCTION

The elastic curved strip can model a seedbed cultivator *s*-tine [1]. Ten variants of *s*-tine finite element models, the shape of which is determined by seven parameters (Fig. 1) have been studied in [2]. In the present paper, we consider an elastic double-spiral strip, which can also model the *s*-tine. The shape of this strip is determined only by two parameters.

The properties of *s*-tines may be determined by natural experiments [3]. Unfortunately, natural experiments are expensive and time consuming. Modern computer software and hardware allow us to make experiments with the finite element models of real *s*-tines. Computer experiments are much cheaper and quicker than natural experiments. Natural experiments may be required to establish the connection between the properties of the real *s*-tine and its finite element model.

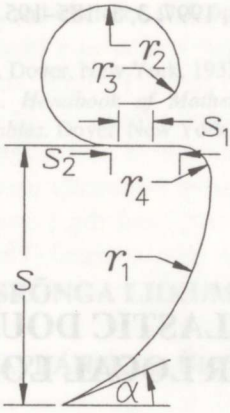


Fig. 1. Shape parameters of the *s*-tine.

The method of computer experiments with the *s*-tine finite element model is used in [1]. We use the same method in this paper.

## 2. GEOMETRY OF THE DOUBLE-SPIRAL STRIP

Let us consider two arcs of spirals determined by the formulas

$$x = \frac{a^{\varphi}\cos(\varphi)}{s}, \qquad y = \frac{a^{\varphi}\cos(\varphi)}{s}, \tag{1}$$

$$x_1 = \frac{b^{\varphi}\cos(\psi)}{s}, \qquad y_1 = \frac{-b^{\varphi}\cos(\psi)}{s}, \tag{2}$$

where $a$, $b$, and $s$ are the parameters of double-spiral arcs, and

$$a\tan[\ln(a)] \le \varphi \le a\tan[\ln(a)] + 2\pi, \qquad a\tan[\ln(b)] \le \psi \le 2\pi .$$

For

$$a = 1.06, b = 1.25, s = 12 \tag{3}$$

the geometric representation of arcs (1) (continuous line) and (2) (dot line) are shown in Fig. 2. By a simple transformation, the arcs (1), (2) are joined into one double-spiral arc. This arc is shown in Fig. 3 for numerical values (3). On the basis of the double-spiral arc, the double-spiral strip is constructed. For the values (3), the finite element model of the strip of the width $d = 0.032$ m is shown in Fig. 4. We assume that one end of this strip is rigidly clamped, and the other one is loaded by force (Fig. 4) on the nodes.

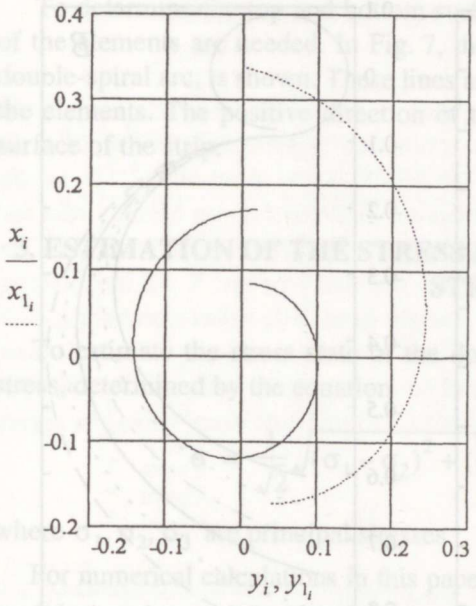


Fig. 2. Initial spiral arcs.

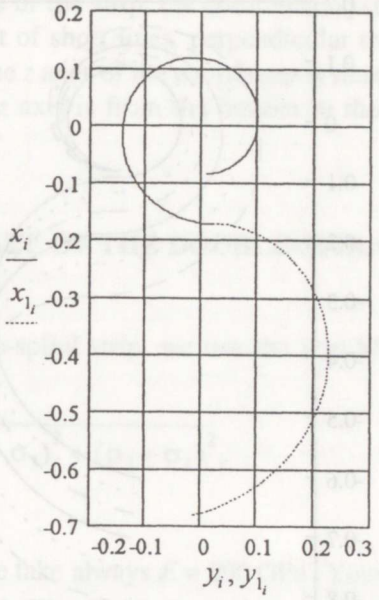


Fig. 3. The double-spiral arc.

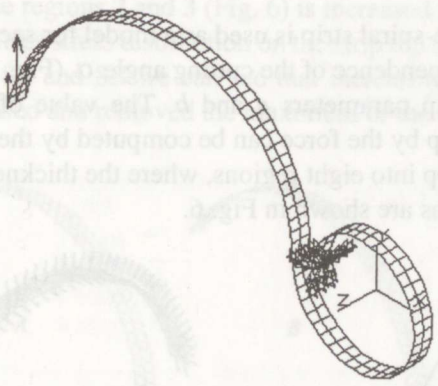


Fig. 4. Force loading and constraints of the double-spiral strip.

Let us consider two sets of double-spiral arcs and the corresponding strips. The first set of arcs is shown in Fig. 5*A*, where the parameters $a$ and $b$ have the values: $a_i = 1.02$; 1.06; 1.10; 1.14; 1.18; 1.22 and $b = 1.25$. The second set of arcs is shown in Fig. 5*B*, where the parameters $a$ and $b$ have the values $a = 1.02$ and $b_i = 1.25$; 1.27; 1.29; 1.31; 1.33; 1.35. (An increment in the parameters $a$ or $b$ results in the increased dimensions of the double-spiral strip.)

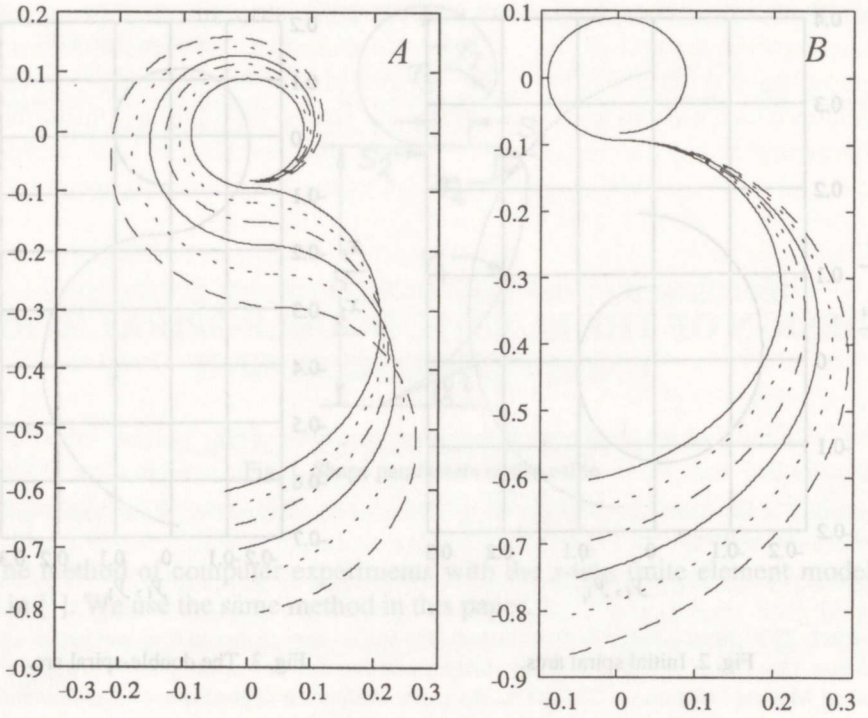


Fig. 5. Sets of double-spiral arcs.

Because the double-spiral strip is used as a model for seedbed cultivator *s*-tine, we studied also the dependence of the cutting angle $\alpha$ (Fig. 1) on the values of the applied force and strip parameters $a$ and $b$. The value of the cutting angle $\alpha$ before loading the strip by the force can be computed by the formula $\alpha = \ln(b)$.

We divided the strip into eight regions, where the thickness of the strip may be different. These regions are shown in Fig. 6.

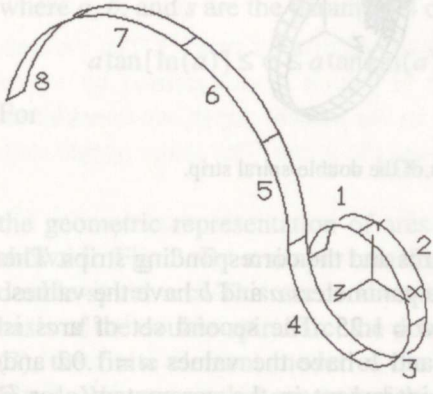


Fig. 6. Regions of the double-spiral strip.

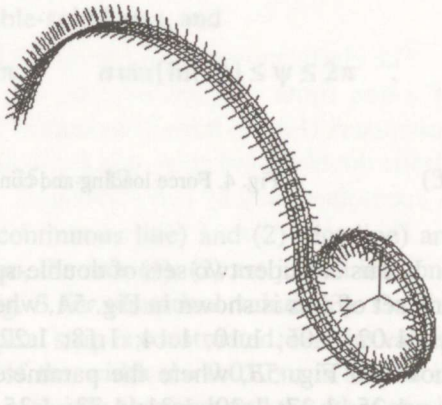


Fig. 7. The element coordinate systems for the finite element model of the double-spiral strip.

To determine the top and bottom surfaces of the strip, the coordinate systems of the elements are needed. In Fig. 7, the set of short lines, perpendicular to the double-spiral arc, is shown. These lines are the $z$ axes of the coordinate systems of the elements. The positive direction of this $z$ axis is from the bottom to the top surface of the strip.

## 3. ESTIMATION OF THE STRESS STATE OF THE DOUBLE-SPIRAL STRIP

To estimate the stress state of the double-spiral strip, we use the von Mises stress, determined by the equation

$$\sigma = \frac{1}{\sqrt{2}}\sqrt{(\sigma_1 - \sigma_2)^2 + (\sigma_2 - \sigma_3)^2 + (\sigma_3 - \sigma_1)^2},$$

where $\sigma_1$, $\sigma_2$, $\sigma_3$ are principal stresses.

For numerical calculations in this paper we take always $E = 200$ GPa (Young's modulus) and $\nu = 0.3$ (Poisson's coefficient). The distribution of the von Mises stress on the strip top surface (Fig. 7), under the load $F = 200$ N in the direction of the global coordinate axis $Y$ (Fig. 4), is shown in Fig. 8*A*. Here, the strips have equal thickness $h = 0.01$ m in all eight regions (Fig. 6) for the values of (3) and $d = 0.032$ m. To decrease the maximum of the von Mises stress in the strip, the thickness of strip in the regions 2 and 3 (Fig. 6) is increased and taken $h = 0.012$ m. In this case, the von Mises stress distribution on the strip top surface is shown in Fig. 8*B*. Comparing Figs. 8*A* and 8*B* we can see that increasing the strip thickness in regions 2 and 3 decreased and removed the maximum of the von Mises stress.

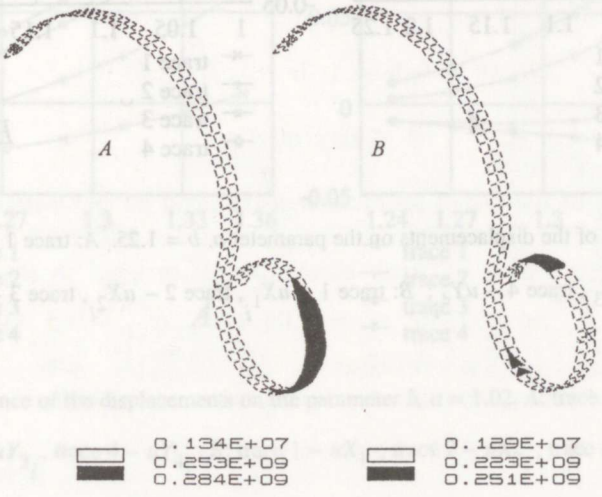


Fig. 8. Distribution of the von Mises stress on the top surface of the double-spiral strip.

## 4. RESULTS OF COMPUTER EXPERIMENTS

Let us consider the results of computer experiments with the strip finite element model, shown in Fig. 8*B*. In the computer experiments, we studied the dependence of displacements *uX*, *uY* (ANSYS 5.0A symbols [4–7]) in the directions of global axes *X* and *Y*, the maximum value of the von Mises stress and the cutting angle $\alpha$ on the values of the total force *F* and parameters *a* and *b*. The experimental values of these parameters are denoted in Figs. 9–12 by different symbols, which for clarity are joined by straight lines. The index numbers 1, 2, 3, and 4 denote the values 200, 400, 600, and 700 N of the total load *F*. For all cases, $s = 12$. Figures 10*A* and 12*A* can be used to choose strip material for seedbed cultivator *s*-tines. Figures 9–12 help to choose seedbed cultivator *s*-tines in regard to agricultural technology.

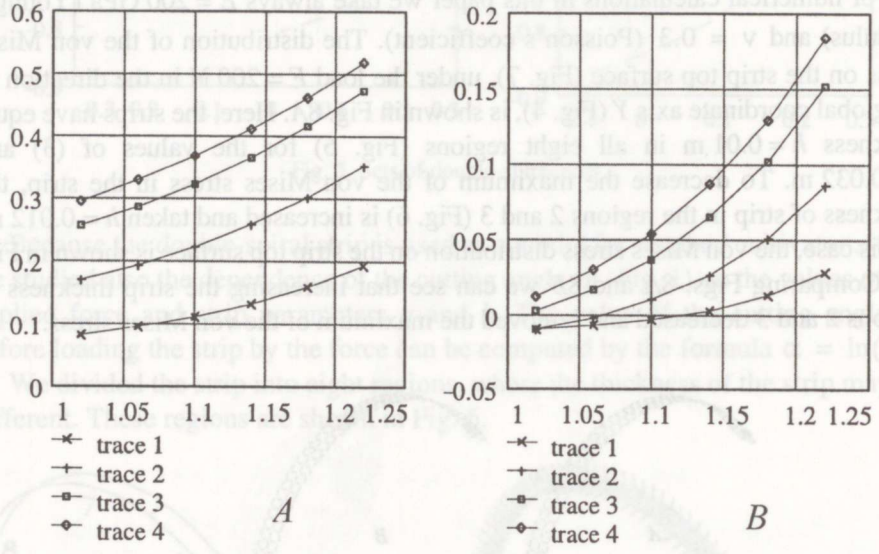


Fig. 9. Dependence of the displacements on the parameter *a*, $b = 1.25$. *A*: trace 1 – $uY_{1_i}$, trace 2 – $uY_{2_i}$, trace 3 – $uY_{3_i}$, trace 4 – $uY_{4_i}$; *B*: trace 1 – $uX_{1_i}$, trace 2 – $uX_{2_i}$, trace 3 – $uX_{3_i}$, trace 4 – $uX_{4_i}$.

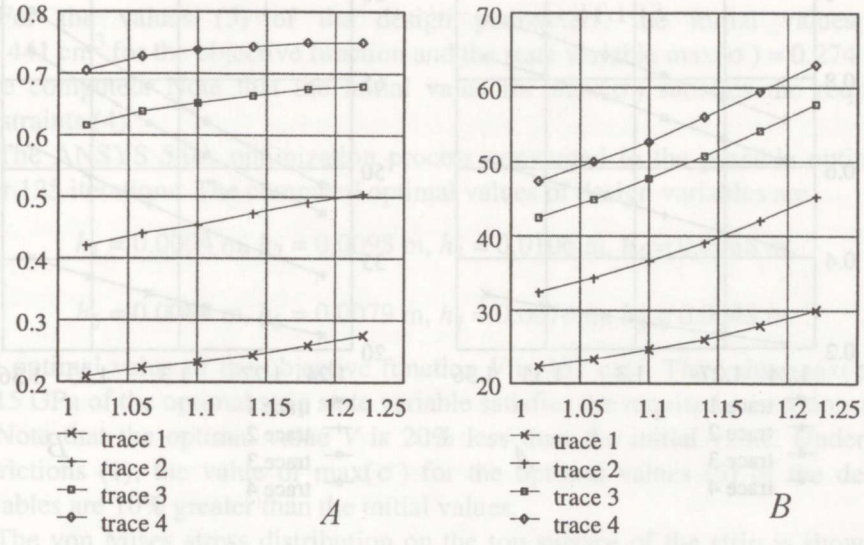


Fig. 10. Dependence of the maximum of the von Mises stress and the cutting angle on the parameter *a*, $b = 1.25$. *A*: trace 1 – $\sigma_{1_i}$, trace 2 – $\sigma_{2_i}$, trace 3 – $\sigma_{3_i}$, trace 4 – $\sigma_{4_i}$; *B*: trace 1 – $\alpha_{1_i}$, trace 2 – $\alpha_{2_i}$, trace 3 – $\alpha_{3_i}$, trace 4 – $\alpha_{4_i}$.

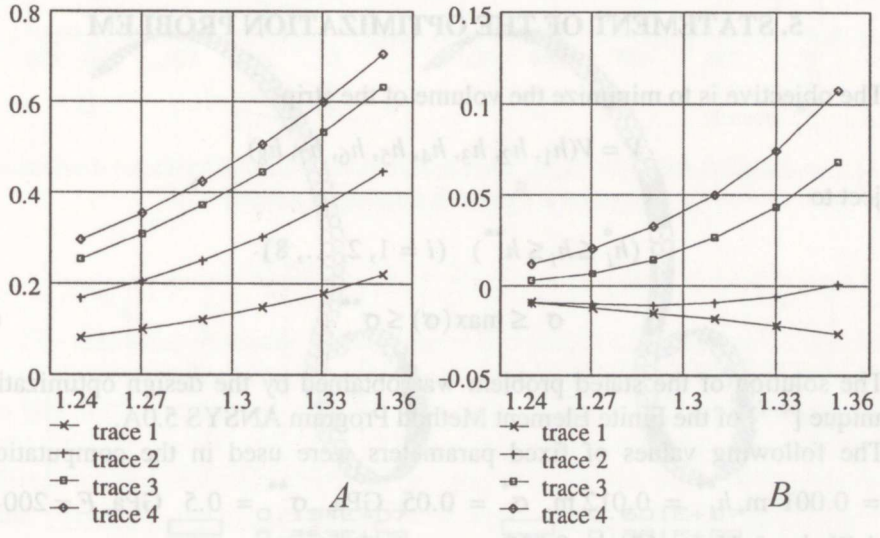


Fig. 11. Dependence of the displacements on the parameter *b*, $a = 1.02$. *A*: trace 1 – $uY_{1_i}$, trace 2 – $uY_{2_i}$, trace 3 – $uY_{3_i}$, trace 4 – $uY_{4_i}$; *B*: trace 1 – $uX_{1_i}$, trace 2 – $uX_{2_i}$, trace 3 – $uX_{3_i}$, trace 4 – $uX_{4_i}$.

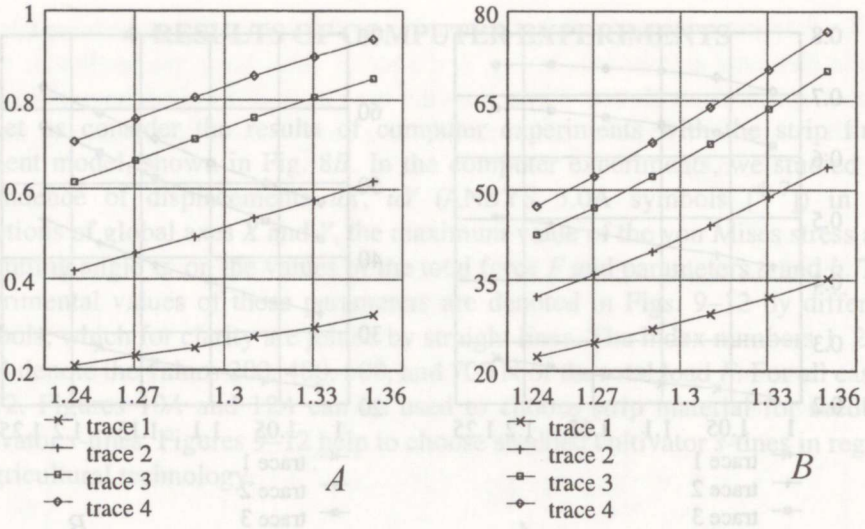


Fig. 12. Dependence of the maximum of the von Mises stress and the cutting angle on the parameter $b$, $a = 1.02$. *A*: trace 1 – $\sigma_{1_i}$, trace 2 – $\sigma_{2_i}$, trace 3 – $\sigma_{3_i}$, trace 4 – $\sigma_{4_i}$; *B*: trace 1 – $\alpha_{1_i}$, trace 2 – $\alpha_{2_i}$, trace 3 – $\alpha_{3_i}$, trace 4 – $\alpha_{4_i}$.

## 5. STATEMENT OF THE OPTIMIZATION PROBLEM

The objective is to minimize the volume of the strip

$$V = V(h_1, h_2, h_3, h_4, h_5, h_6, h_7, h_8)$$

subject to

$$(h_i^* \le h_i \le h_i^{**}) \quad (i = 1, 2, \ldots, 8)$$

$$\sigma^* \le \max(\sigma) \le \sigma^{**} . \tag{4}$$

The solution of the stated problem was obtained by the design optimization technique [4–7] of the Finite Element Method Program ANSYS 5.0A.

The following values of fixed parameters were used in the computations $h_i^* = 0.001$ m, $h_i^{**} = 0.012$ m, $\sigma^* = 0.05$ GPa, $\sigma^{**} = 0.5$ GPa, $F = 200$ N, $a = 1.06$, $b = 1.25$, $s = 12$, $d = 0.032$ m.

For design variables, the following initial values were given

$$h_i = 0.01 \text{ m } (i = 1, 2, \ldots, 8). \tag{5}$$

For the values (5) of the design parameters, the initial values are $V = 441$ cm$^3$ for the objective function and the state variable $\max(\sigma) = 0.274$ GPa were computed. Note that the initial value for $\max(\sigma)$ satisfies the required constraints (4).

The ANSYS 5.0A optimization process converged to the possible optimum after 125 iterations. The computed optimal values of design variables are

$$h_1 = 0.0094 \text{ m}, h_2 = 0.0098 \text{ m}, h_3 = 0.0106 \text{ m}, h_4 = 0.0088 \text{ m},$$
$$h_5 = 0.0084 \text{ m}, h_6 = 0.0079 \text{ m}, h_7 = 0.0070 \text{ m}, h_8 = 0.0048 \text{ m}. \quad (6)$$

The optimal value of the objective function $V$ is 357 cm$^3$. The value $\max(\sigma) = 0.315$ GPa of the optimal strip state variable satisfies the required constraints (4).

Note that the optimal value $V$ is 20% less than the initial value. Under the restrictions (1), the value of $\max(\sigma)$ for the optimal values (6) of the design variables are 10% greater than the initial values.

The von Mises stress distribution on the top surface of the strip is shown in Fig. 13 at the initial (*A*) and optimal (*B*) states. From Fig. 13, one can conclude that these distributions are quite different.

Interestingly, the strip of the minimal volume is "equi-strength", because the maximum of the von Mises stress arises simultaneously at all the regions considered (Fig. 13*B*).

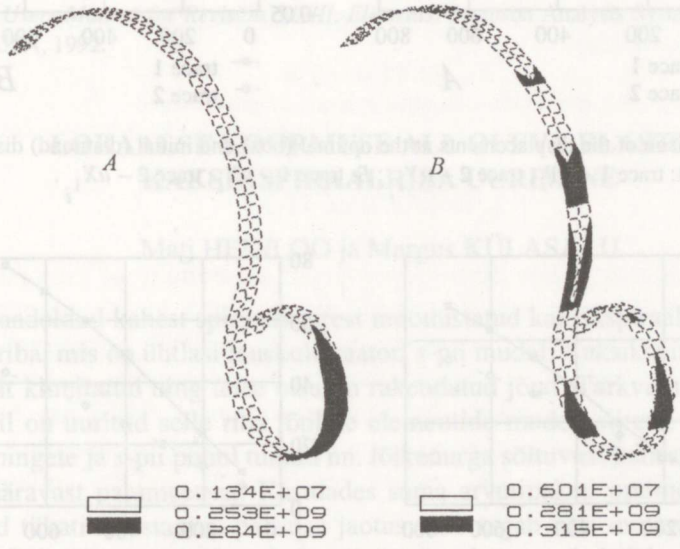


Fig. 13. Distribution of the von Mises stress at the top surface of the double-spiral strip in the initial (*A*) and optimal (*B*) state.

## 6. RESULTS OF COMPUTER EXPERIMENTS ON THE INITIAL AND OPTIMAL STATES OF THE STRIP

Let us compare the results of computer experiments for the initial and optimal distribution of strip thickness under the force values $F = 100, 300, 400, ..., 700$ N. The dependence of displacements in the directions of global axes $X$ and $Y$, the maximum value of the von Mises stress and the cutting angle on the values of the total force $F$ are shown in Figs. 14 and 15. In these figures, the computed numerical values are denoted by different symbols, which for clarity are joined by straight lines. From Fig. 15 one can conclude that with the increase of the force value, the von Mises stress increases for the optimal strip quicker than for the initial strip. Figures 14 and 15*B* show that the flexibility of optimal strip is considerably greater than that of the initial strip. The flexibility is one of the most important characteristics of the seedbed cultivator *s*-tine.

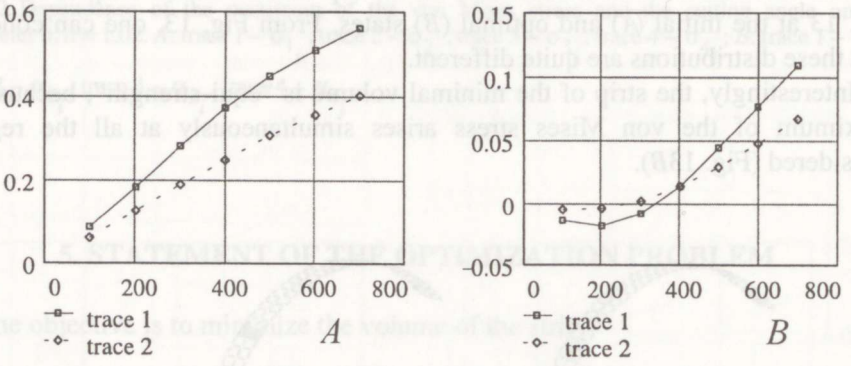


Fig. 14. Comparison of the displacements at the optimal (box) and initial (diamond) distribution of strip thickness. *A*: trace 1 – $uY_i$, trace 2 – $uY_{1_i}$; *B*: trace 1 – $uX_i$, trace 2 – $uX_{1_i}$.

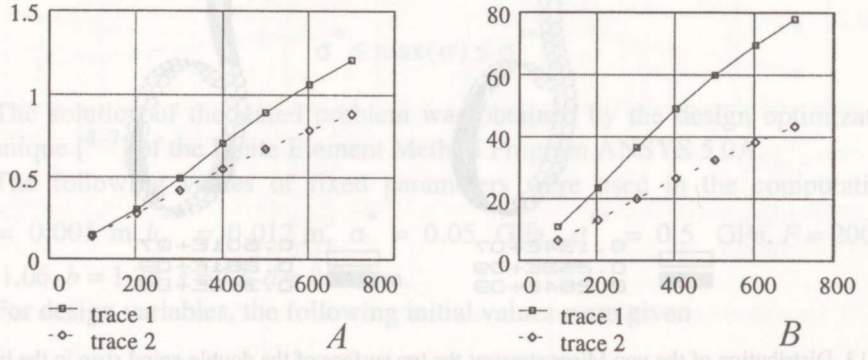


Fig. 15. Comparison of the von Mises stress maxima and the cutting angle at the optimal (box) and initial (diamond) distribution of strip thickness. *A*: trace 1 – $\sigma_i$, trace 2 – $\sigma_{1_i}$; *B*: trace 1 – $\alpha_i$, trace 2 – $\alpha_{1_i}$.

Using the ANSYS 5.0A optimization technique [4–7], we have found the values for design variables, which guarantee the local minimum for the objective function by the redistribution of the stress. One can try to find the other local minimum for the objective function of the new initial values of design variables.

## ACKNOWLEDGEMENT

Support by the Estonian Science Foundation is gratefully appreciated.

## REFERENCES

1. *Spare Parts for Soil Cultivation*. P.D. Rasspe Söhne GmbH&CO KG, 1990.
2. Heinloo, M. and Külasalu, M. Design of seedbed cultivator *s*-tine displacements, soil penetrating angle and maximum equivalent stress under applied load. *Proc. Estonian Agricult. Soc.*, Tartu, 1996, **6**, 4, 389–399 (in Estonian).
3. Viil, E. Applicability of cultivator's *s*-tines to cultivate different soil types. *Proc. Estonian Inst. Agricult. Mechanization*, Saku, 1995, 1, 30–43 (in Estonian).
4. *ANSYS Users Manual for Revision 5.0/IV. Theory*. Swanson Analysis Systems, Inc. Houston, USA, 1992.
5. *ANSYS Users Manual for Revision 5.0/I. Procedures*. Swanson Analysis Systems, Inc. Houston, USA, 1992.
6. *ANSYS Users Manual for Revision 5.0/II. Commands*. Swanson Analysis Systems, Inc. Houston, USA, 1992.
7. *ANSYS Users Manual for Revision 5.0/III. Elements*. Swanson Analysis Systems, Inc. Houston, USA, 1992.

## LOKAALSE KOORMUSE ALL OLEVA ELASTSE KAKSIKSPIRAALRIBA UURIMINE

Mati HEINLOO ja Margus KÜLASALU

On vaadeldud kahest spiraalikaarest moodustatud kaksikspiraali baasil loodud elastset riba, mis on ühtlasi lauskultivaatori *s*-pii mudel. Kaksikspiraalriba üks ots on jäigalt kinnitatud ning teise otsa on rakendatud jõud. Tarkvarapaketi ANSYS 5.0A abil on uuritud selle riba lõplike elementide mudeli siirete, maksimaalsete Misese pingete ja *s*-pii puhul tuntud nn. lõikenurga sõltuvust kahest kaksikspiraali kuju määravast parameetrist. Kasutades sama arvutipaketi optimeerimistehnikat on leitud tükati konstantne paksuse jaotus, mis tagab riba minimaalse ruumala. Misese pinged saavutavad maksimaalväärtuse korraga kaheksas riba etteantud piirkonnas ületamata materjali voolavuspiiri. Minimaalse ruumalaga tükati konstantse paksusega riba mehaanilised omadused erinevad oluliselt konstantse paksusega riba analoogsetest omadustest.